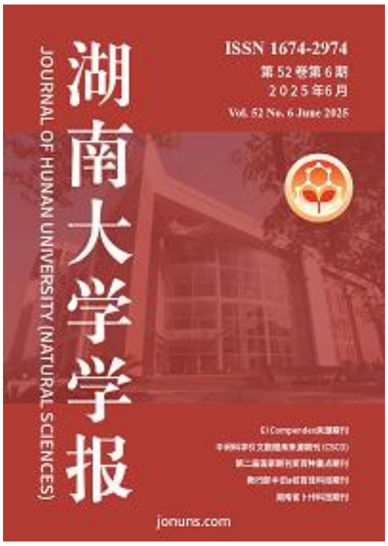

Journal of Hunan University

(Natural Sciences)

Vol. 52 No. 6

June 2025

Available online at

https://jonuns.com

Open Access Article

https://doi.org/10.55463/issn.1674-2974.52.6.5

Osteoporosis Identification Based on Computed Tomography Scan Image and Machine Learning

Maya Genisa [1]*, Johari Yap Abdullah [2]*, Erry Mochamad Arief [3], Bazli Bin MD Yusoff [4], Maman Hermana [5], Chandra Prasetyo Utomo [6]

[1] Biomedical Sciences Program, School of Postgraduate Studies, YARSI University, Jakarta, Indonesia

[2] Craniofacial Imaging Laboratory, School of Dental Sciences, Health Campus, Universiti Sains Malaysia, Kubang Kerian, Kota Bharu 16150, Malaysia and Dental Research Unit, Center for Transdisciplinary Research (CFTR), Saveetha Institute of Medical and Technical Sciences, Saveetha Dental College, Saveetha University, Chennai 602105, India

[3] Periodontic Department, Faculty of Dentistry, AIMST University, Sungai Petani 08100, Malaysia

[4] Radiology Department, Universiti Sains Malaysia, Kubang Kerian, Kota Bharu, Malaysia

[5] Geosciences Department, Faculty of Sciences and Information Technology, Universiti Teknologi PETRONAS, Malaysia

[6] IT Department, YARSI University, Jakarta, Indonesia

* Corresponding authors: maya.genisa@yarsi.ac.id, johariyap@usm.my

Article History:
Received: May 13, 2025
Revised: June 15, 2025
Accepted: July 9, 2025
Published: July 30, 2025

Abstract: Osteoporosis, characterized by a reduction in bone density, is a common condition among the elderly, leading to increased fracture risks. Early detection is critical for effective medical intervention to prevent severe complications. This study explores the viability of using machine learning-based technologies for detecting osteoporosis through computerized tomography (CT) scan images and enhanced image attributes. The machine learning model was trained on a dataset of 520 CT scan images from patients with normal and osteoporotic bone conditions.

Novel image attributes – phase, contrast, roughness, and grayscale – were derived from the original CT scan images. These attributes were tested in multiple input scenarios (single, double, and multi-attribute) to assess their contribution to the accuracy of the model. The results demonstrated that incorporating these image attributes into the machine learning model significantly enhanced the detection accuracy of osteoporosis, showcasing the potential of this method for automated, non-invasive diagnosis. Unlike conventional methods, this approach introduces a novel set of image attributes for bone quality evaluation, which improves the prediction of osteoporosis in CT scan images and reduces false negatives. However, further validation on a larger dataset is required before clinical application.

Keywords: Osteoporosis, Bone Quality, Imaging, CT-Scan, Automatization.

基于计算机断层扫描图像和机器学习的骨质疏松症识别

摘要：骨质疏松症是老年人群的常见疾病，其特征是骨密度降低，导致骨折风险增加。早期发现对于有效的医疗干预和预防严重并发症至关重要。本研究探索了利用机器学习技术通过计算机断层扫描 (CT) 图像和增强图像属性检测骨质疏松症的可行性。该机器学习模型基于 520 幅来自正常和骨质疏松症患者的 CT 扫描图像数据集进行训练。从原始 CT 扫描图像中衍生出新的图像属性——相位、对比度、粗糙度和灰度。这些属性在多种输入场景（单属性、双属性和多属性）下进行测试，以评估其对模型准确性的贡献。结果表明，将这些图像属性纳入机器学习模型可显著提高骨质疏松症的检测准确性，展现了该方法在自动化、非侵入性诊断方面的潜力。与传统方法不同，该方法引入了一套用于骨质量评估的新型图像属性，从而提高了 CT 扫描图像中骨质疏松症的预测能力，并降低了假阴性率。然而，在临床应用之前需要对更大的数据集进行进一步验证。

关键词：骨质疏松症、骨质量、成像、CT扫描、自动化.

1. Introduction

The growing elderly population presents increasing challenges for healthcare systems, including the age-related decline in bone quality. Osteoporosis, a condition characterized by reduced bone density and increased susceptibility to fractures, is highly prevalent among older adults. Although not directly life-threatening, osteoporosis can lead to serious complications if fractures occur without timely medical intervention. Therefore, early detection of osteoporosis enables the prompt initiation of appropriate therapeutic measures. As a result, early diagnosis and intervention can effectively prevent the adverse consequences associated with this condition.

However, early detection of osteoporosis remains challenging. Bone mineral density (BMD) measurement, which is typically the primary indicator of bone health, is often not performed due to limited availability of required equipment. Dual-energy X-ray absorptiometry (DXA) is the most widely used method for assessing BMD. Nevertheless, DXA is not always accessible in smaller or rural healthcare settings. Moreover, the diagnostic interpretation based on DXA can be complicated by various factors, including image acquisition protocols, post-processing techniques, analytical variability, image artifacts, and potential diagnostic pitfalls [1]. Additional patient-specific factors—such as ethnicity, sex, and body composition—must also be taken into account when evaluating bone quality [2].

This article investigates the feasibility of integrating machine learning with alternative imaging modalities – specifically, computed tomography (CT) scan images – to quantify bone quality, with a focus on differentiating between osteoporotic and healthy bone. Recent advances in machine learning have enabled its widespread application across various domains, including medicine. Albuquerque et al. [3] classified bone conditions using supervised machine learning based on electromagnetic wave recordings. Their results demonstrated that combining electromagnetic sensing with machine learning can effectively indicate osteoporosis status, offering advantages such as reduced cost and shorter processing time.

In this study, we aim to advance existing approaches by exploring imaging modalities other than DXA for osteoporosis assessment. We propose the development of novel image-based features and their integration into machine learning models to enable automated classification of bone health.

2. Bone Quality Assessment

Bone is a dynamic tissue composed of cells responsible for both resorption and formation. In a healthy individual, these processes are in equilibrium.

However, when this balance is disrupted; for example, when the rate of bone resorption exceeds that of bone formation, substantial bone loss occurs, leading to a decline in bone quality. This imbalance is characteristic of osteoporosis, a condition in which bone resorption predominates over remodeling.

The extent of bone remodeling is influenced by the internal surface area available for cellular activity. Cortical bone has a relatively low surface area compared to trabecular bone, which is highly porous and metabolically more active. Consequently, trabecular bone exhibits greater changes in bone mineral density (BMD) and is more susceptible to osteoporotic deterioration than cortical bone [4].

Figure 1 illustrates bone structure in CT images of a normal bone (Figure 1a) and an osteoporotic bone (Figure 1b). In CT imaging, higher radiodensity corresponds to brighter (whiter) regions, indicating harder, denser bone, while darker areas represent lower density and reduced hardness. The grayscale intensity, expressed in Hounsfield units (HU), is directly related to bone mineral density. Qualitatively, bone structure in CT images is assessed by evaluating HU values or grayscale intensity as a visual indicator of bone density.

(a)

(b)

Figure 1. CT scan images of (a) normal bone and (b) osteoporosis bone (authors' scan images)

Eventually, dual-energy X-ray absorptiometry (DXA) became the gold standard for measuring bone mineral density. However, DXA has several limitations, including relatively high radiation exposure in certain protocols, difficulties in accurately reconstructing fracture morphology, and reduced sensitivity in detecting subtle fractures and structural changes. To address these limitations, Yaprak et al. [5] proposed the use of CT-derived Hounsfield units (HU) as a practical and accessible method for osteoporosis assessment.

The use of computed tomography (CT) scan images as a screening tool for osteoporosis has also been explored in clinical contexts such as chronic pancreatitis and other systemic conditions [6]. Variations in bone quality and microstructure not only result in distinct HU values but may also affect other image-based features concealed within the CT data. Genisa et al. [7] successfully identified several image attributes, extracted through image processing techniques, that can differentiate between healthy and osteoporotic bone using original CT scan images.

Figure 2 illustrates examples of image attributes (specifically, grayscale contrast features) derived from CT images. A notable difference is evident between healthy bone (Figure 2a) and osteoporotic bone (Figure 2b) within the regions enclosed by red circles. The magnitude of the image attribute is quantified by an attribute index. In this example, contrast-based features were used, revealing that normal bone exhibits a lower index value compared to osteoporotic bone.

(a)

(b)

Figure 2. Example of image attribute derived from computed tomography (CT) scan data on the pelvis (red circle). (a) Original CT image of normal bone, and (b) original CT image of osteoporosis bone, circle) [7].

The application of machine learning to automate bone assessment has been explored in various studies, with differing levels of performance. Rahim et al. [8] evaluated the accuracy of existing machine learning techniques in detecting osteoporosis using DXA images. Their results demonstrated that machine learning achieves a satisfactory level of diagnostic accuracy, with some models also showing improvement in fracture prediction.

Sebro and Elmahdy [9] utilized computed tomography (CT) scan images as input for a machine learning algorithm designed to detect knee osteoporosis and osteopenia. Their findings indicated that opportunistic screening for low bone density can be effectively performed using routine CT scans combined with machine learning. Sebro and Ramos [10] extended this approach by applying machine learning to CT imaging for the detection of cervical spine osteoporosis. Their method successfully classified bone conditions and incorporated Hounsfield unit (HU) thresholding into the analysis of CT images.

Although DXA remains the gold standard for assessing bone mineral density (BMD) and diagnosing osteoporosis, alternative imaging modalities—such as MRI, quantitative CT (qCT), optical coherence tomography (oCT), and others—offer viable options for bone quality evaluation. These modalities may provide advantages in terms of accessibility, cost, and integration into existing clinical workflows [11].

3. Method

The methodology employed in this study is an image processing and machine learning–based approach for detecting osteoporosis using computed tomography (CT) scan images. To evaluate the feasibility of applying machine learning to CT images for osteoporosis identification, a dataset of 520 CT scans, comprising cases of both normal and osteoporotic bone, was used to train and test the classification algorithm.

The original CT images contain multiple tissue types. Therefore, a segmentation process was performed to isolate bone tissue and exclude non-skeletal structures. Segmentation was conducted in two stages: first, a Hounsfield unit (HU) threshold was applied to extract mineralized bone based on radiodensity; this was followed by morphological operations to refine the segmentation and retain only the anatomically relevant bone regions of interest.

Figure 3 illustrates the pelvic region before and after segmentation, demonstrating the effectiveness of the isolation process.

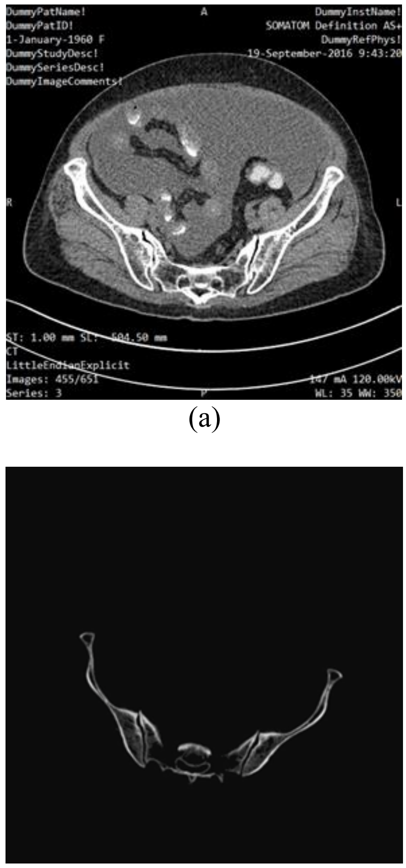

(a)

(b)

Figure 3. Segmented pelvic bone: (a) before and (b) after segmentation (authors' scan images)

Four image attributes – Grayscale (derived from the original CT image), Roughness, Grayscale Contrast, and Phase were extracted using signal processing techniques. To quantify the intensity of each attribute, an attribute index was formulated as a scalar measure representing its magnitude within the region of interest (ROI).

3.1. Grayscale Index (GI)

In CT imaging, tissue density and hardness are represented by Hounsfield units (HU). Bone assessment is performed within a user-defined region of interest (ROI), selected based on anatomical relevance. The strength of the grayscale attribute is determined by computing the average HU value within the ROI.

The Grayscale Index (GI) is defined as the root mean square (RMS) of the HU values in the specified ROI, providing a robust measure of average bone density that is less sensitive to noise than a simple arithmetic mean. The GI is calculated using Equation (1):

$$GI = \sqrt{\frac{1}{N}\sum_{n=1}^{N} HU^2} \quad (1)$$

3.2. Roughness Index (RI)

The roughness attribute quantifies local heterogeneity in bone texture within the region of interest (ROI). It is derived by calculating the deviation of individual Hounsfield unit (HU) values from the mean HU within the ROI, reflecting variations in bone density at the voxel level. This attribute captures microarchitectural irregularities associated with trabecular degradation in osteoporosis.

The Roughness Index (RI) is computed as the root mean square of these deviations, providing a measure of textural complexity. The formulation is given by Equation (2):

$$RI = HU_i - \frac{1}{N}\sum_{i=1}^{N} HU_i \, , \qquad (2)$$

where HU is the HU value of a pixel at a certain region of interest.

3.3. Contrast Index (CI)

The Contrast Index (CI) is computed to quantify the magnitude of local intensity variations in CT images, reflecting spatial changes in radiodensity. Since CT images represent the X-ray attenuation properties of tissues, the CI serves as an indicator of the heterogeneity in absorption across adjacent regions. Higher contrast values correspond to sharper transitions in density, which are typically associated with preserved trabecular architecture, while lower values may indicate structural degradation seen in osteoporosis.

The CI is derived from the first-order derivative of the Hounsfield unit (HU) intensity field within the region of interest (ROI), capturing the rate of change in attenuation. This gradient-based measure emphasizes edges and textural boundaries in the bone structure. Equation (3) illustrates the discrete formulation of the CI:

$$CI = \left[\frac{\sum_{k=-K}^{+K}\left(\left[\frac{\partial a_{jk}}{\partial x}\right]^2 + \left[\frac{\partial a_{jk}}{\partial y}\right]^2\right)}{\sum_{k=-K}^{+K}\sum_{j=1}^{j} a_{jk}^2}\right]^{1/2}, \quad (3)$$

where the a_{jk} denotes the HU value in two dimensions at the pixel, where x and y are the coordinates; CI represents the contrast of HU caused by the absorption or intensity of X-ray energy.

3.4. Phase Index (PI)

To determine the Phase Index (PI), the image is subjected to a 2D Fourier transform. The initial step involves converting the original image to a complex number via the Hilbert transform, which is defined by Equation (4). The phase index, which is equivalent to the phase difference between the image's real and imaginary components, is computed using Equation (5).

$$\emptyset(x, y) = arc\ Tan\left(\frac{\{HT(x,y)\}}{HT(x,y)}\right) \qquad (4)$$

$$CI = \left[\frac{\sum_{k=-K}^{+K}\left(\left[\frac{\partial a_{jk}}{\partial x}\right]^2 + \left[\frac{\partial a_{jk}}{\partial y}\right]^2\right)}{\sum_{k=-K}^{+K}\sum_{j=1}^{j} a_{jk}^2}\right]^{1/2} \qquad (5)$$

In the given context, HU represents the HU value of the pixel denoted by x and y, HT denotes the Hilbert transform, and $\emptyset(x, y)$ signifies the phase. The index term is calculated for all image attributes by dividing the normalized value of each attribute by the number of pixels comprising the region of interest.

The classification or automation of bone assessment is accomplished through machine learning using a convolutional neural network (CNN) architecture. A diagrammatic representation of the bone classification process is illustrated in Figure 4. The input features for this algorithm consist of image attributes derived from the original CT scan data. Three distinct scenarios were executed to evaluate the benefits of using attributes to enhance the accuracy of machine learning in identifying bone conditions: single attribute, double attribute, and multi-attribute. The AI/ML algorithm's performance is evaluated by assessing output accuracy, including the identification of true positives, true negatives, false positives, and false negatives.

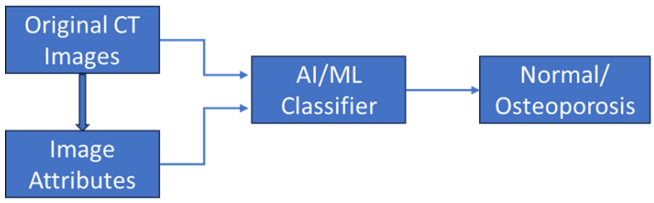

Figure 4. AI/ML workflow for bone classification (developed by the authors)

4. Results and Discussion

4.1. Image Attribute Analysis

A quick examination of the images is sufficient to perform a diagnosis of the bone condition, provided that the image accurately depicts the condition. Nonetheless, this method is often subjective. As a result, quantitative analysis is typically required. One approach to determining the quantitative value is to calculate the index number. In the future, this value may serve as a benchmark or reference for establishing the conditions. The evaluated images derived from CT scans are listed below along with their corresponding index numbers. The investigation focused on the pelvic bone, an additional site of osteoporosis prevalent among the elderly.

4.2. Grayscale Index (GI)

The HU on the CT image denotes the tissues' hardness. However, various factors can influence the HU in CT, some of which may not directly reflect the condition of the material. These factors vary depending on the specific equipment and dosage used. Therefore, the direct threshold of HU for indicating bone density must be carefully considered. Grayscale values for bone are greater than those of soft tissues. Bones with greater density are expected to exhibit higher grayscale values than those with lower density. Bone density estimated by computed tomography correlates strongly with BMD.

Kim et al. [12] demonstrated that the HU may serve as a criterion for assessing bone condition.

To obtain the Grayscale Index (GI), an average value is calculated within a specific region of interest. Figure 5 illustrates the applied grayscale attributes of normal and osteoporotic pelvic bones. The ROI is denoted by the red line. Normal bone has a higher GI value than bone with osteoporosis.

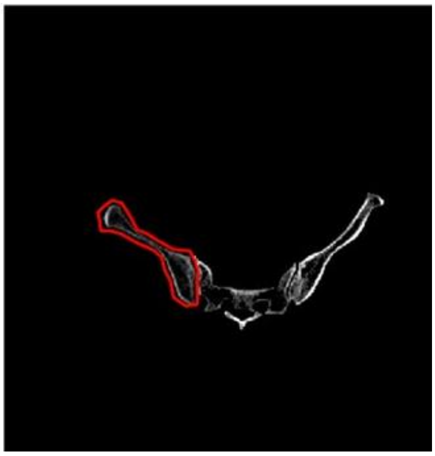

Gray index = 71
(a)

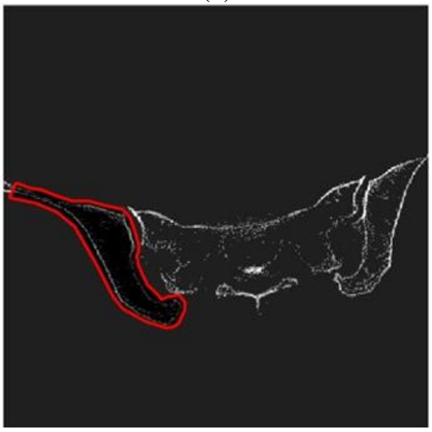

Gray index = 29
(b)

Figure 5. Illustrates the Grayscale Index computed on (a) the original CT scan image of normal bone and (b) the original CT scan image of bone with osteoporosis (authors' scan images)

4.3. Roughness Index (RI)

Bones vary in density and microstructure throughout their composition. Due to the modeling and remodeling process, bone heterogeneity can be increased [13]. The Roughness Index (RI) of various bone conditions was computed in this investigation. However, the evaluation region included both cortical and trabecular bone. As shown in Figure 6, the new image attribute of roughness is calculated for both normal and osteoporotic conditions. The RI value of normal bone is higher than that of osteoporotic bone. Visually, in the roughness attribute, normal bone has a denser appearance than bone with osteoporosis, particularly in the cortical region.

Roughness index = 56
(a)

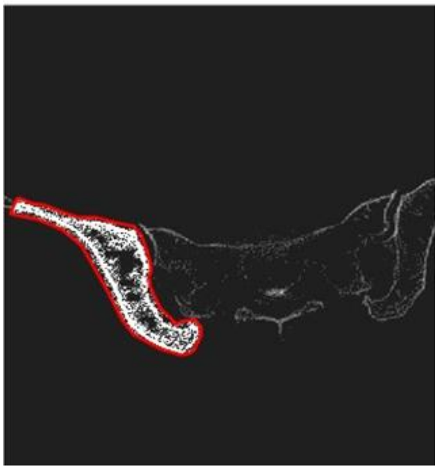

Roughness index = 44
(b)

Figure 6. Roughness Index of bone on the: (a) normal and (b) osteoporosis conditions (authors' scan images)

4.4. Contrast Index (CI)

Bone resorption and remodeling processes tend to increase the heterogeneity of bone density and bone mineral density (BMD). Not only do they impact the overall density of bone minerals, but they also influence the density distribution. Furthermore, it is possible that BMDD could serve as a metric for assessing bone health [14]. The Contrast Index (CI) indicates the difference in HU between the current pixel and the adjacent pixel. A greater magnitude of density variation results in higher contrast. In the case of osteoporosis, where bone heterogeneity is substantial, a high CI is expected. CI applied to CT scan images is illustrated in Figure 7. The results indicate that the CI value of osteoporotic bone is higher than that of normal bone. As hypothesized, bones with osteoporosis are observed to have a progressive increase in BMDD rather than a decrease in BMD. A possible correlation exists between high BMDD variability and elevated bone fracture risk.

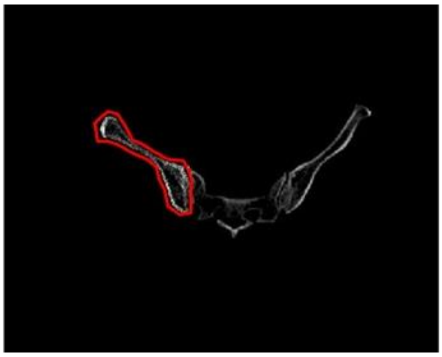

Contrast index = 38

(a)

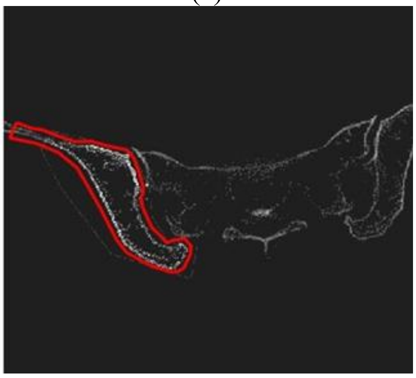

Contrast index = 63

(b)

Figure 7. Contrast index at two bone types: (a) normal and (b) osteoporosis (authors' scan images)

4.5. Phase Index (PI)

Formation takes place on outer surfaces as a compensatory measure for bone loss, while resorption predominates on inner surfaces in the elderly. Bone quality deteriorates when the processes of resorption and remodeling are unbalanced, as is the case in osteoporosis. This mechanism is mediated by osteoblasts and osteoclasts. The inability of osteoblasts to function results in the failure to generate collagen molecules, which can lead to skeletal fragility. Thus, the remodeling process influences the structural integrity and metabolic capabilities of the skeleton. The trabecular bone structure becomes finer in individuals with osteoporosis, whereas cortical bone porosity increases. The phase attributes and bone structure of osteoporotic and normal bone were compared using scanning electron micrographs obtained from biopsies [13]. This is illustrated in Figure 8. The phase index of denser bone structures is higher than that of thinner bone structures in osteoporotic bone.

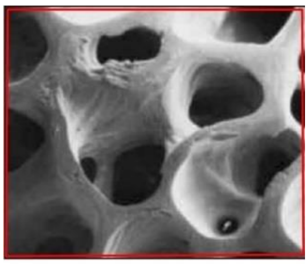

(a)

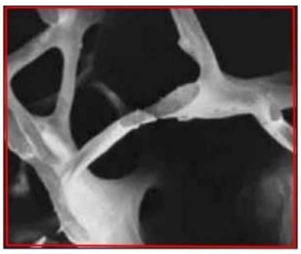

(b)

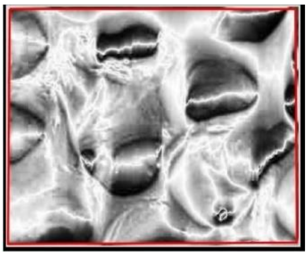

Phase index=67

(c)

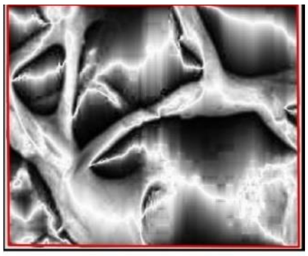

Phase index=33

(d)

Figure 8. A phase index comparison of the bone structure of healthy and osteoporosis-affected individuals. (a) Normal bone, (b) osteoporosis bone, (c) normal bone phase attribute, and (d) osteoporosis bone phase attribute (authors' scan images)

Applying the phase attribute to the CT scan images of the pelvic bone is shown in Figure 9. It is obvious that the normal pelvic bones and osteoporosis bone have different appearances. Phase index value. The phase index of normal bone (PI = 66) was higher than that of osteoporosis (PI = 34). Generally, the PI value decreases from normal bone to osteoporosis bone.

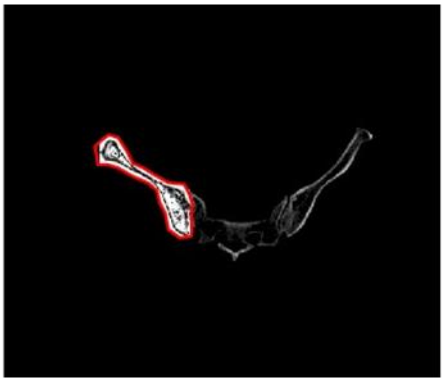

Phase Index = 66

(a)

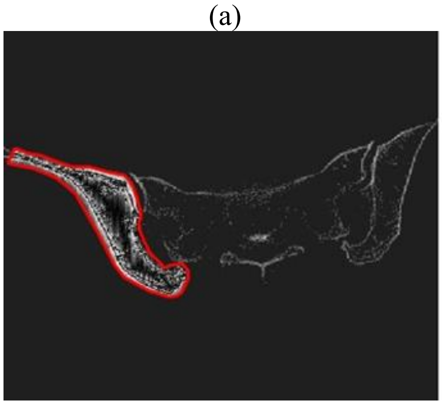

Phase Index = 34

(b)

Figure 9. Illustrates the Phase Index of (a) normal, and (b) osteoporosis bone (authors' scan images)

4.6. Visual Comparison

The qualitative diagnosis of osteoporosis can be aided by visual distinctions between osteoporotic and healthy bone. Thus, before conducting quantitative analysis, it is preferable to have an image attribute that can differentiate osteoporosis from healthy bone for rapid visual inspection. The following summarizes the evaluated image characteristics of the pelvic bone compared with the initial CT scan image (Figure 10).

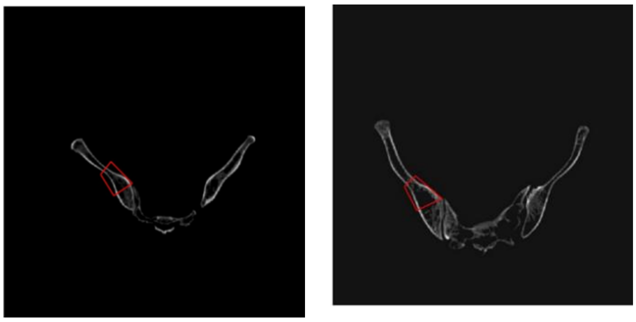

(a)

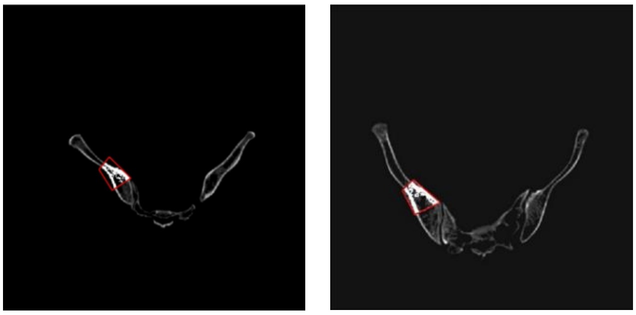

(b)

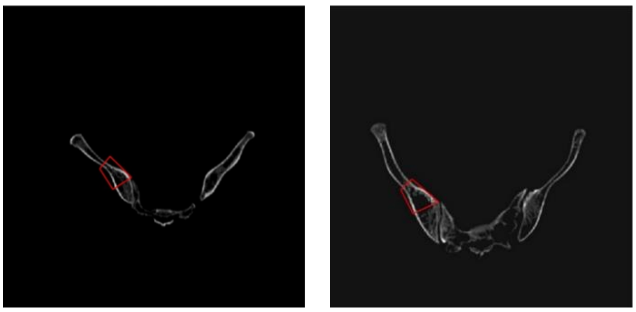

(c)

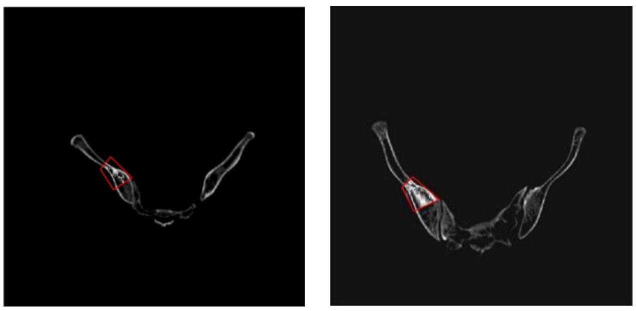

(d)

Figure 10. Visual comparison of various attributes of normal bone (left) and osteoporosis (right) of (a) original computed tomography scan (grayscale), (b) roughness, (c) contrast, and (d) phase attribute (authors' scan images)

4.7. Implementation of AI/ML for Osteoporosis Evaluation

An alternative approach to mitigate the subjectivity associated with image-based osteoporosis diagnosis is to automate the process using a machine learning algorithm. However, the precision and dependability of this method require further investigation. The present study documents the application of ML techniques in the context of image-based bone diagnosis.

The effectiveness of machine learning diagnoses is assessed through prediction accuracy and the loss function. Accuracy signifies the degree to which machine learning can approximate the true condition, whereas the loss function reflects prediction errors when the model fails to identify the true condition. Two types of prediction errors are distinguished: false positives and false negatives. A false positive occurs when a condition is erroneously diagnosed despite its absence. A false negative, on the other hand, refers to an erroneous diagnosis in which the condition is present but not detected by ML. Although the primary objective of machine learning diagnosis is to achieve high accuracy, the loss function remains indispensable. In medical applications, reducing false negatives is more critical than reducing false positives.

To evaluate the efficacy of ML, three distinct test scenarios involving single attributes, double attributes, and multiple attributes were executed. In the single attribute scenario, the ML model is trained using one attribute. An example of a single image attribute, such as the original CT image, is employed as input for the AI/ML algorithm. In the double-attribute scenario, the input to the AI/ML algorithm consists of a pair comprising one derived attribute and the original CT scan, or two derived attributes. In contrast, in the multi-attribute scenario, the input consists of all attributes in addition to the original CT scan. With the sole distinction being the input, each test was executed using the same machine learning architecture and the same dataset. The training dataset comprised 160 healthy bone samples and 160 osteoporosis-affected bone samples. Ten bone samples were used in the testing phase: five normal bones and five with osteoporosis; these samples were excluded from the training phase.

Test of a single attribute: This experiment aimed to determine the efficacy of each attribute in automatically detecting osteoporosis via machine learning. For each of these machine learning inputs – contrast, roughness, phase, and CT – the input consists of a single value. Figure 11 illustrates the efficacy of machine learning using a CT image and a single attribute; results are also presented in Figure 11. During the training phase, the machine accurately predicted the target bone with a loss function of approximately 10% and 100% accuracy. When presented with new data samples, the AI/ML model's ability to correctly identify the target deteriorated; it correctly predicted 60% of cases, with the remaining 40% classified as false negatives. Four out of five bones affected by osteoporosis were misclassified as normal. Table 1 summarizes the accuracy of each attribute. The findings indicate that the roughness attribute yields the highest accuracy at 100%, whereas the original CT image results in the falsest negatives.

Table 1. Performance of AI/ML in predicting bone condition using a single attribute (compiled by the authors)

Attribute	True Positive	True Negative	False Positive	False Negative
CT	50%	10%	0	40%
Roughness	50%	50%	0	0
Contrast	50%	10%	40%	0
Phase	50%	20%	0	30%

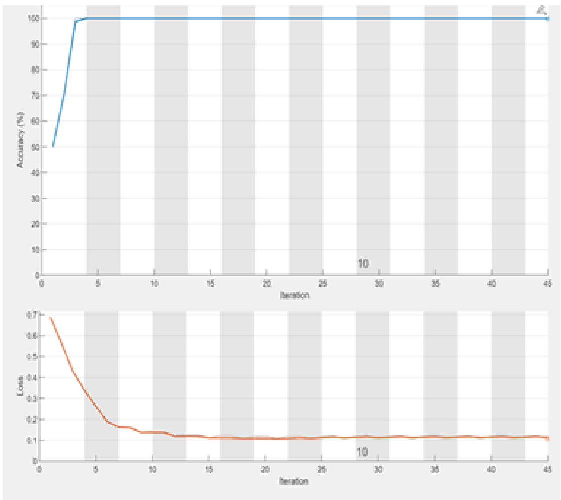

(a)

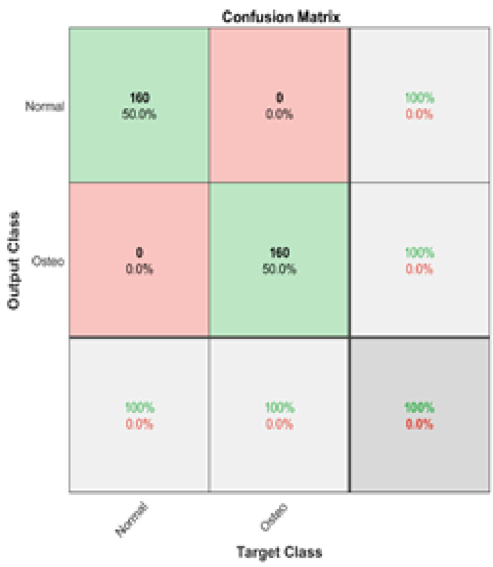

(b)

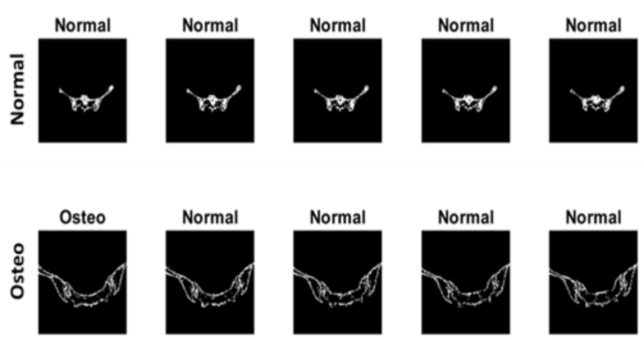

(c)

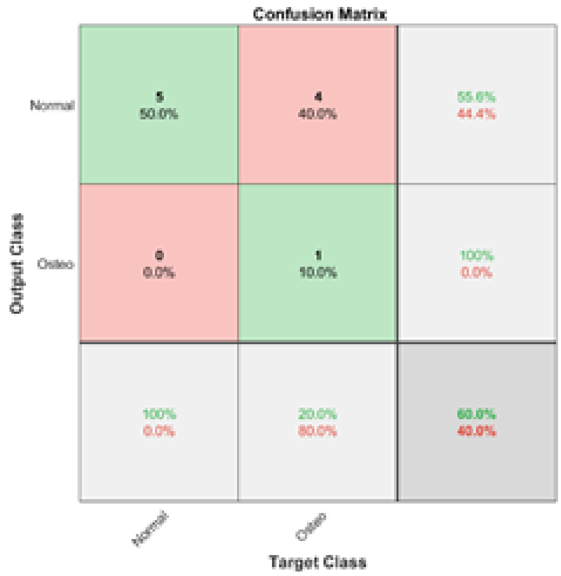

(d)

Figure 11. The efficacy of AI/ML using only CT scan images was trained on hundreds of data samples. (a) Accuracy and loss function, (b) confusion matrix at the training stage, (c) predicted output, and (d) confusion matrix of the output (test stage on 10 samples) (authors' design)

For the double-attribute test, the input was initialized with a pair of attributes. In addition to testing the original CT scan paired with another attribute, alternative attribute pairs without CT were also examined. Figure 12 displays the outcome of the CT–roughness attribute pair, and Table 2 summarizes the results for the remaining pairings. The use of paired attributes improved the predictive accuracy of ML for osteoporosis. The accuracy of the CT pair with roughness attributes is identical to that of the CT pair with phase attributes: 100%. However, CT continues to produce a 30% false negative rate when combined with contrast and phase attributes.

Table 2. Performance of AI/ML in predicting bone condition using pair attributes (compiled by the authors)

Attribute Pair	True Positive	True Negative	False Positive	False Negative
CT-Roughness	50%	50%	0	0
CT- Contrast	50%	20%	0	30%
CT-Phase	50%	20%	0	30%
Roughness-Phase	50%	50%	0	0

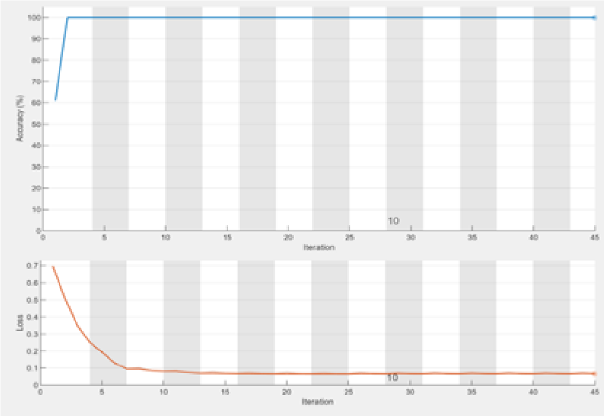

(a)

(b)

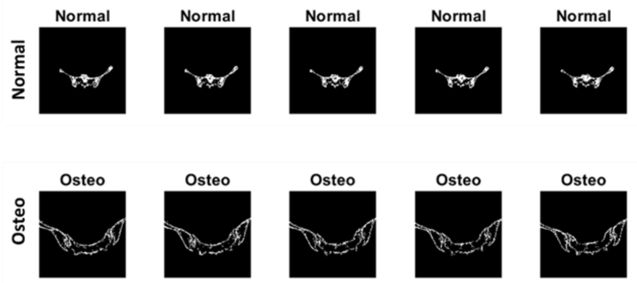

(c)

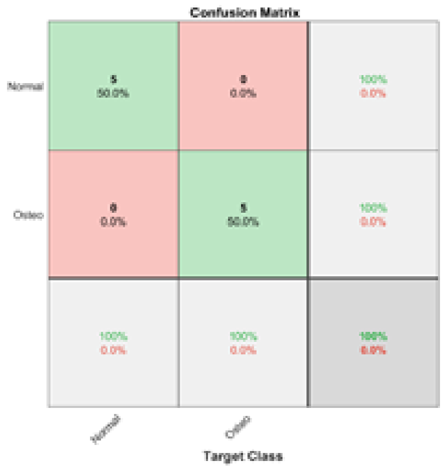

(d)

Figure 12. The efficacy of AI/ML using only computed tomography scan images: (a) accuracy and loss function, (b) confusion matrix at the training stage, (c) predicted output, and (d) confusion matrix of the output (test stage) (authors' design)

The multi-attributes test was executed by providing the AI/ML algorithm with CT and all attributes as inputs. The outcome indicates that the highest lev-el precision (100%) was attained. Every single targeted bone was accurately predicted, and the loss function was maintained at 10% (Figure 13).

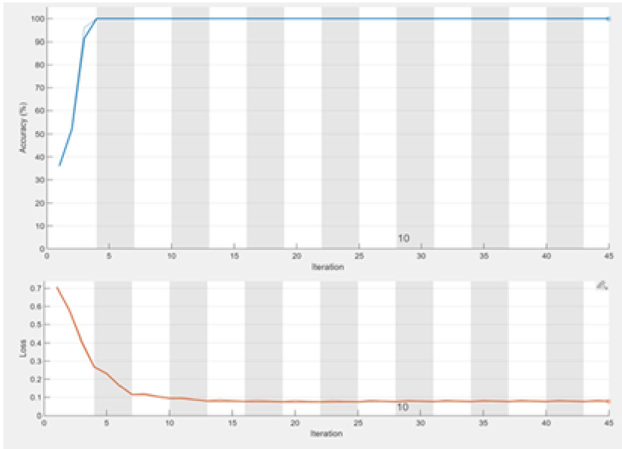

(a)

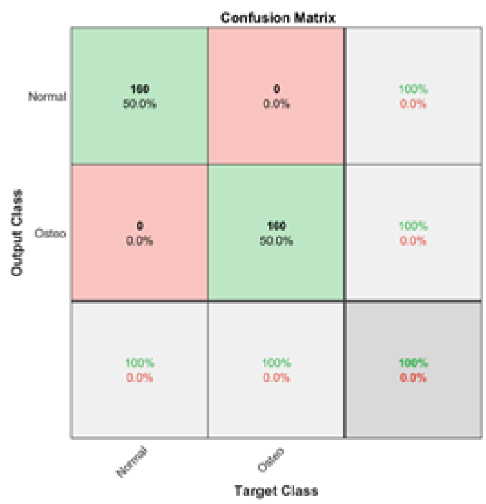

(b)

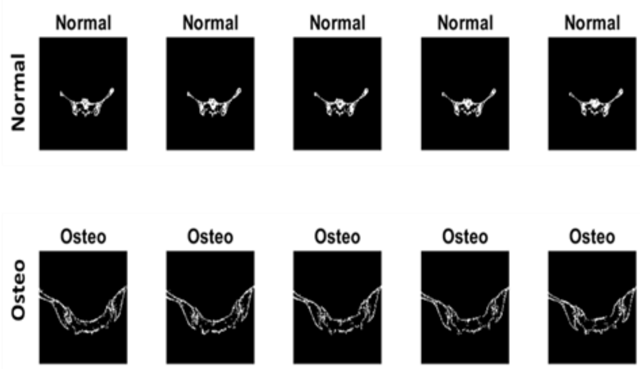

(c)

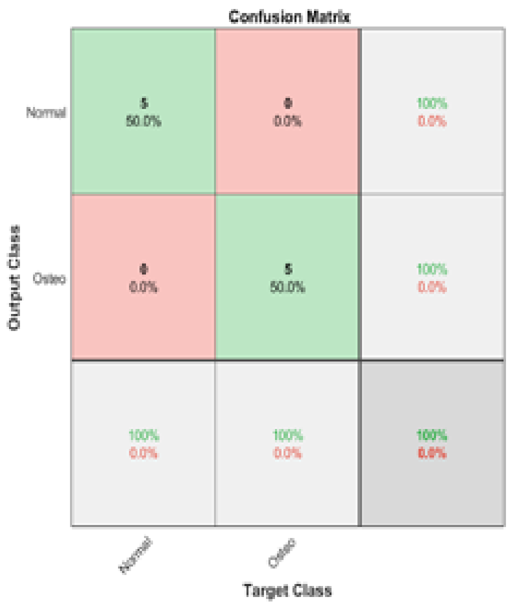

(d)

Figure 13 illustrates the performance of AI/ML with multiple attributes: (a) accuracy and loss function, (b) confusion matrix at the training stage, (c) predicted output, and (d) confusion matrix of the output (test stage) (authors' design)

5. Conclusion

Osteoporosis is the most prevalent condition among the elderly and necessitates timely intervention to prevent severe complications. Nevertheless, early detection of osteoporosis remains challenging and is often limited to a single technique. This research presents an alternative approach to detecting osteoporosis from computed tomography (CT) scan images by employing advanced image processing methods and artificial intelligence/machine learning technology. Four image attributes—namely, grayscale, roughness, contrast, and phase—were developed and tested. The roughness and phase characteristics of osteoporosis-affected bone differ significantly from those of healthy bone. However, the use of these characteristics as supplementary features in ML models can enhance the accuracy of AI/ML in the automated detection of osteoporosis. In contrast to relying solely on CT scan images, incorporating additional attributes as input can improve accuracy and reduce the occurrence of false negatives in prediction outcomes. This approach can serve as an alternative method for distinguishing osteoporosis from healthy bone or for detecting the condition.

This study presents an innovative approach for osteoporosis detection using machine learning techniques and novel image attributes derived from computed tomography scans, such as grayscale, roughness, contrast, and phase. These attributes, which are essential for accurate diagnosis, improve detection accuracy and reduce false negative errors. By combining image processing and machine learning, this method offers a faster and more cost-effective non-invasive alternative to traditional techniques such as DXA. The main innovation of this study is the use of multiple image attributes to enhance the accuracy and efficiency of osteoporosis detection.

Based on the findings, this machine learning–based method is recommended for osteoporosis detection in clinical settings where DXA is not readily accessible. Future efforts should focus on further validation of the model using larger and more diverse datasets to confirm its generalizability across different populations. Moreover, integrating this automated detection system into clinical practice would significantly reduce the burden on healthcare professionals, enabling faster and more accurate diagnoses.

The next steps in this research should involve refining the model to achieve higher accuracy and incorporating additional image attributes that may further enhance the evaluation of bone condition. Future studies could also explore combining different imaging modalities, such as MRI or qCT, with machine learning to provide a comprehensive and robust diagnostic tool. Additionally, real-time application of the model in clinical settings, followed by longitudinal studies to monitor its impact on patient outcomes, would help establish the method's clinical utility and effectiveness.

Declarations

Author Contributions:

Conceptualization, J.Y.A. and M.G.; methodology, J.Y.A.; software, M.H.; validation, J.Y.A., E.M.A., and C.P.U.; formal analysis, M.H.; investigation, M.G., and B.B.Y..; resources, M.G., and J.Y.A.; data curation, E.M.A., and B.M.Y.; writing—original draft preparation, all authors contributed equally; writing—review and editing, J.Y.A. and E.M.A.; visualization, E.M.A., B.B.Y. and C.P.U.; supervision, M.G.; project administration, J.Y.A. All authors have read and agreed to the published version of the manuscript.

Data Availability Statement

The data presented in this study are available on request from the corresponding author.

Acknowledgments

This research was funded by a grant from the Ministry of Higher Education of Indonesia (Contract Number: 1160/LL3/AL.04/2023), and the APC was partly funded by Re-search Grant: YUTP-FRG (015LC0-504).

Conflicts of Interest

The authors declare no conflicts of interest.

References

[1] BANKS K.P., FARRELL M.B., GUNTHER R.S., MCWHORTER N.E., BYERLY D.W., and PEACOCK J. G. Improving DXA quality by avoiding common technical and diagnostic pitfalls: Part 1. *Journal of Nuclear Medicine*

Technology, 2023, 51(3): 167–175. https://doi.org/10.2967/jnmt.122.264885

[2] NELSON D.A., PETTIFOR J.M., & NORRIS S.A. Race, ethnicity and osteoporosis. In: MARCUS, R., FIELDMAN, D., NELSON, D. & ROSEN, C. (eds). *Osteoporosis*. 3rd ed. San Diego: Elsevier, 2008: 667-687. http://hdl.handle.net/20.500.11910/4492

[3] ALBUQUERQUE G. A., CARVALHO D. D. A., CRUZ A. S., SANTOS J. P. Q., MACHADO G. M., …, & LIMA J. Osteoporosis screening using machine learning and electromagnetic waves. *Scientific Reports*, 2023, 13(1): 12865. https://doi.org/10.1038/s41598-023-40104-w

[4] HASELTINE K. N., CHUKIR T., SMITH P. J., JACOB J. T., BILEZIKIAN J. P., and FAROOKI A. Bone mineral density: clinical relevance and quantitative assessment. *Journal of Nuclear Medicine*, 2021, 62(4): 446–454. https://doi.org/10.2967/jnumed.120.256180

[5] YAPRAK G., GEMICI C., SESEOGULLARI O. O., KARABAG I. S., and CINI N. CT derived Hounsfield unit: an easy way to determine osteoporosis and radiation related fracture risk in irradiated patients. *Frontiers in Oncology*, 2020, 10: 742. https://doi.org/10.3389/fonc.2020.00742

[6] MCNABB-BALTAR J., MANICKAVASAGAN H. R., CONWELL D. L., LU A., YADAV D., … & SHAH Z. K. A pilot study to assess opportunistic use of CT-scan for osteoporosis screening in chronic pancreatitis. *Frontiers in Physiology*, 2022, 13: 866945. https://doi.org/10.3389/fphys.2022.866945

[7] GENISA M., ABDULLAH J. Y., YUSOFF B. M. D., ARIEF E. M., HERMANA M., and UTOMO C. P. Adopting signal processing technique for osteoporosis detection based on CT scan image. *Applies Sciences*, 2023, 13(8): 5094. https://doi.org/10.3390/app13085094

[8] RAHIM F., ZAKI ZADEH A., JAVANMARDI P., EMMANUEL KOMOLAFE T., KHALAFI M., … & SHIRBANDI K. Machine learning algorithms for diagnosis of hip bone osteoporosis: A systematic review and meta-analysis study. *Biomedical Engineering Online*, 2023, 22(1): 68. https://doi.org/10.1186/s12938-023-01132-9

[9] SEBRO R., and ELMAHDY M. Machine learning for opportunistic screening for osteoporosis and osteopenia using knee CT scans. *Canadian Association of Radiologists Journal*, 2023, 74(4): 676–687. https://doi.org/10.1177/08465371231164743

[10] SEBRO R., and DE LA GARZA-RAMOS C. Utilizing machine learning for opportunistic screening for low BMD using CT scans of the cervical spine. *Journal of Neuroradiology*, 2023, 50(3): 293–301. https://doi.org/10.1016/j.neurad.2022.08.001

[11] DESHPANDE N., HADI M. S., LILLARD J. C., PASSIAS P. G., LINZEY J. R., SAADEH Y. S., LABAGNARA, M. & PARK, P. Alternatives to DEXA for the assessment of bone density: a systematic review of the literature and future recommendations. *Journal of Neurosurgery. Spine*, 2023, 38(4): 436–445. https://doi.org/10.3171/2022.11.spine22875

[12] KIM Y.S., LEE S., SUNG Y.K., & LEE B.G. Assessment of osteoporosis using pelvic diagnostic computed tomography. *Journal of Bone and Mineral Metabolism* , 2016, 34(4): 457–463. https://doi.org/10.1007/s00774-015-0684-0

[13] Office of the Surgeon General (US). Bone health and osteoporosis: a report of the Surgeon General. US Department of Health and Human Services, 2004.

[14] ROSCHGER P., PASCHALIS E.P., FRATZL P., & KLAUSHOFER K. Bone mineralization density distribution in health and disease. *Bone*, 2008, 42(3): 456–466. https://doi.org/10.1016/j.bone.2007.10.021

参考文:

[1] BANKS K.P.、FARRELL M.B.、GUNTHER R.S.、MCWHORTER N.E.、BYERLY D.W. 和 PEACOCK J. G. 通过避免常见的技术和诊断陷阱来提高 DXA 质量：第一部分。《核医学技术杂志》，2023，51(3): 167–175。https://doi.org/10.2967/jnmt.122.264885

[2] NELSON D.A.、PETTIFOR J.M. 和 NORRIS S.A. 种族、民族和骨质疏松症。引自：MARCUS, R.、FIELDMAN, D.、NELSON, D. 和 ROSEN, C. (eds)。骨质疏松症。第 3 版。圣地亚哥：爱思唯尔，2008：667-687。 http://hdl.handle.net/20.500.11910/4492

[3] ALBUQUERQUE G. A.、CARVALHO D. D. A.、CRUZ A. S.、SANTOS J. P. Q.、MACHADO G. M.、…和 LIMA J. 使用机器学习和电磁波进行骨质疏松症筛查。《科学报告》，2023，13(1): 12865。https://doi.org/10.1038/s41598-023-40104-w

[4] HASELTINE K. N.、CHUKIR T.、SMITH P. J.、JACOB J. T.、BILEZIKIAN J. P. 和 FAROOKI A. 骨矿物质密度：临床相关性和定量评估。《核医学杂志》，2021，62(4): 446–454。https://doi.org/10.2967/jnumed.120.256180

[5] YAPRAK G.、GEMICI C.、SESEOGULLARI O. O.、KARABAG I. S. 和 CINI N. CT 衍生的亨斯菲尔德单位：一种确定受放射治疗患者骨质疏松症和放射相关骨折风险的简便方法。 肿瘤学前沿，2020，10: 742. https://doi.org/10.3389/fonc.2020.00742

[6] MCNABB-BALTAR J.、MANICKAVASAGAN H. R.、CONWELL D. L.、LU A.、YADAV D.、… 和 SHAH Z. K. 一项评估 CT 扫描在慢性胰腺炎骨质疏松症筛查中机会性应用的初步研究。 生理学前沿，2022，13: 866945. https://doi.org/10.3389/fphys.2022.866945

[7] GENISA M., ABDULLAH J. Y., YUSOFF B. M. D., ARIEF E. M., HERMANA M., 和 UTOMO C. P. 采用信号处理技术基于 CT 扫描图像检测骨质疏松症。应用科学，2023，13(8): 5094。https://doi.org/10.3390/app13085094

[8] RAHIM F.、ZAKI ZADEH A.、JAVANMARDI P.、EMMANUEL KOMOLAFE T.、KHALAFI M. 和 SHIRBANDI K. 用于诊断髋骨骨质疏松症的机器学习算法：一项系统综述和荟萃分析研究。生物医学工程在线，2023，22(1): 68。https://doi.org/10.1186/s12938-023-01132-9

[9] SEBRO R. 和 ELMAHDY M. 使用膝关节 CT 扫描进行

骨质疏松症和骨质减少机会性筛查的机器学习。加拿大放射学会杂志，2023，74(4): 676–687。https://doi.org/10.1177/08465371231164743
[10] SEBRO R. 和 DE LA GARZA-RAMOS C. 利用机器学习对颈椎CT扫描中的低骨密度进行机会性筛查。《神经放射学杂志》，2023，50(3): 293–301。https://doi.org/10.1016/j.neurad.2022.08.001
[11] DESHPANDE N.、HADI M. S.、LILLARD J. C.、PASSIAS P. G.、LINZEY J. R.、SAADEH Y. S.、LABAGNARA, M. 和 PARK, P. DEXA 评估骨密度的替代方案：文献系统综述和未来建议。《神经外科杂志》。脊柱，2023，38(4): 436–445。https://doi.org/10.3171/2022.11.spine22875
[12] KIM Y.S.、LEE S.、SUNG Y.K. 和 LEE B.G. 使用盆腔诊断性 CT 评估骨质疏松症。《骨与矿物质代谢杂志》，2016，34(4): 457–463。https://doi.org/10.1007/s00774-015-0684-0
[13] 美国卫生局局长办公室。《骨骼健康与骨质疏松症：卫生局局长报告》。美国卫生与公众服务部, 2004。
[14] ROSCHGER P.、PASCHALIS E.P.、FRATZL P. 和 KLAUSHOFER K. 健康和疾病状态下的骨矿化密度分布。《骨》，2008，42(3): 456–466。https://doi.org/10.1016/j.bone.2007.10.021

Word count (excluding references): 6,639 words.

Peer-review record:

- ***Fast-track status:*** Not fast-tracked
- ***First-round reviews received:*** 3 reports
- ***Revision cycles completed:*** 3 rounds
- ***Final version submitted:*** July 9, 2025

Disclaimer/Publisher’s Note: